

Organic Reactions in the Solid State: Reactions of Enclathrated 3,4-Epoxycyclopentanone (= 6-Oxabicyclo[3.1.0]hexan-3-one) in Tri-*o*-thymotide and Absolute Configuration of 4-Hydroxy- and 4-Chlorocyclopent-2-en-1-one

by Raymond Gerdil*, Huiyou Liu¹), and Gérald Bernardinelli

Department of Organic Chemistry and Laboratory of X-Ray Crystallography, University of Geneva, CH-1211 Geneva 4

Several aspects of the heterogeneous actions of aqueous and gaseous HCl on the chemical behavior of 3,4-epoxycyclopentanone (= 6-oxabicyclo[3.1.0]hexan-3-one; **1**) included in the asymmetric cages of tri-*o*-thymotide (TOT) clathrates belonging to space groups $P3_121$ are described, showing specific features strikingly at variance with those observed in liquid solutions. In a first step, the substrate underwent an acid-promoted allylic isomerization, as already observed in our previous investigations, to give optically active 4-hydroxycyclopent-2-en-1-one (**2**). In a consecutive step, a displacement of the OH group was accomplished by the Cl⁻ anion to afford the corresponding chloro compound **3**. Polymorphism was encountered in the preparation of TOT/**1** clathrates. Recrystallization of TOT in the pure guest **1** yielded micro-twinned crystals belonging to the $P3_1$ space group (host/guest ratio 1 : 1), whereas the expected $P3_121$ lattice grew from a mixture of TOT, **1**, and MeOH. The structural determination of TOT/**1** was carried out by X-ray diffraction (Fig. 1). Kinetic measurements were achieved that shed light on some striking features of this type of heterogeneous reactions for solid-liquid and solid-gas systems. Several reactions of pure clathrate antipodes (+)-TOT/**1** with gaseous HCl were carried out under various conditions; concentration and enantiomer-excess(ee) determinations of the products **2** and **3** allowed to establish a larger ee for **3**, thus demonstrating the influence of the host-guest diastereomeric association on the progression of the reaction. The correlation of optical activities of the host and products for the global reaction disclosed the sequence (+)-(*M*)-TOT/**1** → (-)-**2** → (-)-**3**. A new way for the preparation of **2** was devised. It was further demonstrated that the X-ray structure analysis of the chiral clathrate (*M*)-TOT/(+)-**2** (Fig. 4) associated with chiroptical measurements was an efficient and straightforward method to determine the absolute (+)-(*R*)-configuration of the guest. The enantioselectivity of the TOT clathrate for **2** was established by two different methods which allowed the appraisal of an accurate revised value of the specific rotation of **2**. The enclathration of **3** occurred exclusively in the orthorhombic centrosymmetric host lattice $Pbca$, thus prohibiting the X-ray structural determination of the guest absolute configuration. The problem of finding a pathway to the intended enantiomer enrichment of **3** was worked out through the action of aqueous HCl on microcrystalline (+)-TOT/(-)-(*S*)-**2** that gave an optically active mixture of unreacted **2** with **3** as sole product. The pure optically active **3** was isolated by subsequent TLC. The resolution of **3** was achieved by GC over a chiral column and its (unknown) specific rotation measured. The absolute configuration of **3** was established by the measurement of the enantiomer purity of the optically active mixture **3** obtained after the total conversion of (-)-(*S*)-**2** in the presence of thionyl chloride in Et₂O, dioxane, and benzene. It was deduced that the (-)-**3** enantiomer had the (*S*)-configuration.

1. Introduction. – Tri-*o*-thymotide (= 1,7,13-trimethyl-4,10,16-tris(1-methylethyl)-6*H*,12*H*,18*H*-tribenzo[*b,f,j*][1,5,9]trioxacyclododecin-6,12,18-trione; TOT; Fig. 1) has become known as a versatile clathrate host crystallizing in 12 different space groups.

¹) The results presented hereafter are parts of the Ph.D. Thesis of *H.L.* (Thèse No. 2702, Université de Genève).

The TOT clathrates that have aroused most interest are chiral and of enantiomorphous space group $P3_121$, where any single crystal displays either only (P) or only (M) helicity for the host molecule. These types of clathrate crystallize under spontaneous resolution providing discrete C_2 cavities that allow guest chiral discrimination. An extensive review of this particular aspect of enclathration with respect to TOT, as well of its applications, has been recently published [1].

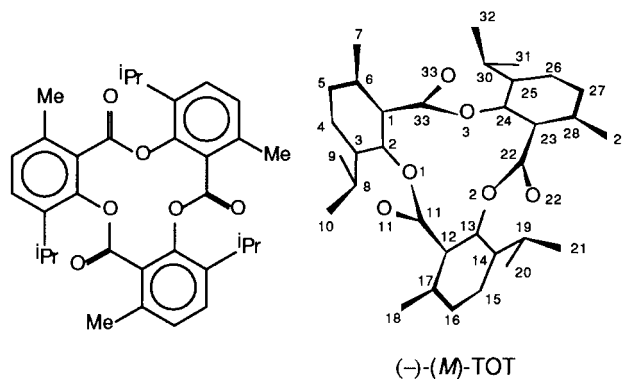
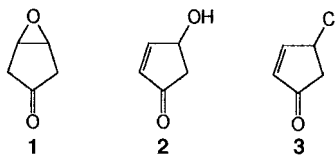


Fig. 1. *Tri-o-thymotide* constitution and idealized view of the (-)-(M)-TOT configuration. The atom numbering (arbitrary) refers to that used in the crystal-structure determinations.

Gerdil and *Barchietto* have reported that the heterogeneous interaction of a series of enclathrated oxirane derivatives with gaseous hydrogen halides (HX_g) and aqueous hydrogen halide solutions (HX_{aq}) exhibited regio- or stereospecific asymmetric reactions of the guests [2]. The hydrogen halide ($X = Cl, Br$) can permeate the crystalline phase and react with the included guest without interfering chemically with the host lattice. Most of the observed processes consist of two consecutive transformations. First, a specific *allylic isomerization* of the oxirane occurs, followed by either one of two paths depending on the substrate: a *nucleophilic substitution* of the allylic OH group leading to an α,β -unsaturated halide, or the *addition* of hydrogen halide to the double bond to form the corresponding halohydrin. The allylic isomerization in the solid-state differs strikingly from the corresponding ring-opening occurring in the homogeneous acidic phase where no traces of allylic product or unsaturated halide can be detected.

In contrast to the exhaustive study of TOT-enclathrated oxiranes with HX_g and HX_{aq} , there had been no attempt to examine the cage-controlled reactivity of the related epoxy ketone system. Epoxy ketones have aroused interest as synthetic intermediates because of their facile preparation, often with substantial stereochemical control, and their enhanced reactivity in acid- and base-catalyzed reactions as well as in other transformations [3]. The present publication continues our preceding studies, examining the cage-controlled chemical behavior of 3,4-epoxycyclopentanone (= 6-oxabicyclo[3.1.0]hexan-3-one; **1**) with the same reactants under similar conditions. The choice of **1** as an epoxy ketone was also dictated by its small size that must fit the cage volume, the latter being a rather constant property of TOT $P3_121$ clathrates.



2. Reactions of Enclathrated 3,4-Epoxy cyclopentanone (1) with HCl. Kinetics and Configuration Correlations. – The epoxy ketone **1** was obtained by peroxidation of cyclopent-3-en-1-one using trifluoroperacetic acid in CH_2Cl_2 [4]. Single and microcrystals of TOT/**1** were prepared following the general procedure described in [2]. Micro-twinned clathrate crystals (space group $P3_1$, host/guest stoichiometric ratio 1:1) were obtained by recrystallization of TOT in the pure guest **1**, whereas the expected lattice $P3_121$ grew from a mixture of TOT, **1**, and MeOH²⁾ and had an occupation ratio of 0.52–0.66, a below-average value for this type of clathrate. Optically active microcrystalline samples were prepared by seeding and proved to be 99% enantiomerically pure. The X-ray structure of TOT/**1** was determined with a single crystal grown from a slowly cooled TOT solution in a mixture of **1** and MeOH (volume ratio 1:2). As depicted in Fig. 2, the guest five-membered ring is approximately parallel to the vertical twofold axis (not shown), with the carbonyl group pointing towards the origin.

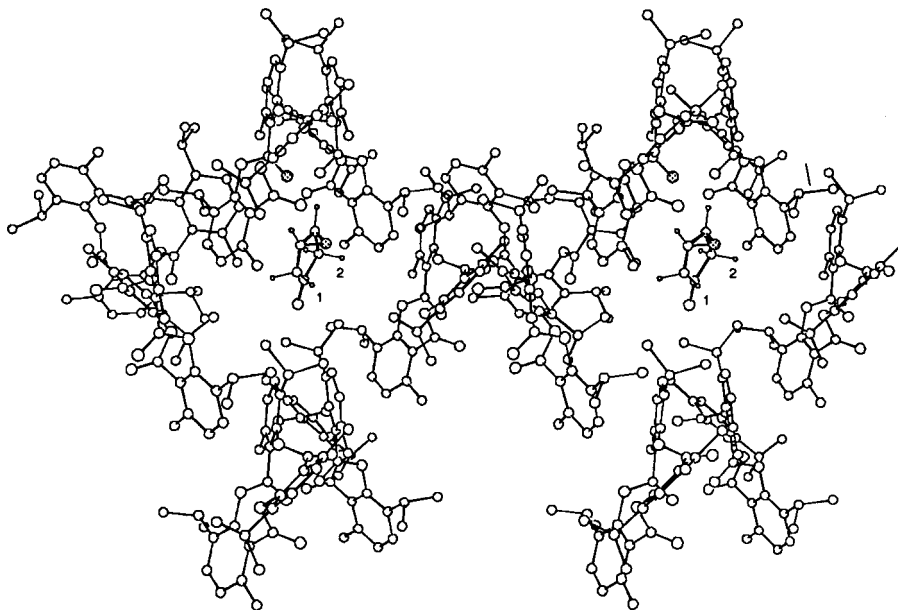
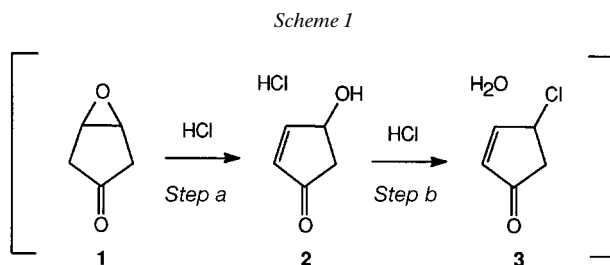


Fig. 2. Stereoview of the (M)-TOT/3,4-epoxycyclopentanone (**1**) clathrate structure ($P3_121$) comprising the host molecules bordering the cavity. For clarity, the top right TOT molecule has been removed. The crystallographic twofold axis passing through the cage lies parallel with the vertical b axis (not shown). The guest is viewed across the 'entry channel' as discussed in Sect. 2. Only the H-atoms of the guest are shown. The solid filled O-atoms are H-bonded as shown in TOT/**2**, on opening of the epoxy ring.

²⁾ The molecular volume of MeOH is too small to allow facile inclusion of the molecule.

To acquire a view on the kinetic aspects of the intracrystalline conversion of **1** under the action of HCl, a series of reactions was performed under various conditions. The ensuing results may allow one to make some choice among plausible mechanisms within the cage. Reactions of enclathrated **1** were investigated for heterogeneous solid-gas and solid-liquid systems. In the first system, microcrystalline conglomerates were reacted in a gas flow of anhydrous HCl (HCl_g); in the second, a suspension of microcrystals was gently stirred in an aqueous solution of HCl (HCl_{aq}). It was found that the reaction involves cage-specific isomerization of the guest **1** to the corresponding allylic alcohol 4-hydroxy cyclopent-2-en-1-one (**2**) in a first step (*Scheme 1, Step a*), followed by nucleophilic substitution of the OH group (*Step b*) leading to the α,β -unsaturated halide **3** (for convenience, enclosed molecules are depicted in square brackets).



The molecular ratios of the starting material and products were determined by peak integration of $^1\text{H-NMR}$ spectra and expressed as dimensionless relative concentrations in the calculations. Microcrystalline conglomerates were used in the measurements, entailing the absence of discrimination between diastereoisomeric reaction paths. As a result, the observed kinetic parameters must be considered as average values. All things being equal, the average flux of H^+Cl^- into the crystal lattice is supposed to be constant for a given weight of microcrystals. It is reminded that the kinetic parameters depend implicitly on the average size of the microcrystals (*i.e.*, on the mean solid-phase area per unit weight of microcrystals) that has been shown to be reproducible throughout treatment of kinetic data owing to the standardized method of preparation. The rate constants were calculated by minimizing the sum of squares ($\sum \text{err}^2$) of the difference between the variations in observed relative concentrations and those calculated on the basis of the integrated form of the assumed rate law [5]. Concentration-time measurements were achieved in the *solid-liquid* system at different HCl_{aq} concentrations and fixed temperatures. Kinetic data were rationalized in terms of rate expressions applied to liquid solutions, revealing remarkable analogies with the latter, as also disclosed in [2]. A concentration-time profile is depicted in *Fig. 3,a* for the reaction carried out at 40° . The kinetic behavior agrees well with the occurrence of two successive first-order (or pseudo-first-order) steps such as $\mathbf{1} - k_1 \rightarrow \mathbf{2} - k_2 \rightarrow \mathbf{3}$ (*Scheme 1*). The bimolecularity of the reaction is substantiated by the steric confinement imposed by the cage upon the reactants. However, in both steps, the concentration of HCl may assume a 'constant' unitary value on account of the cage enclosure, as reflected in the order of the reaction. The rates (in h^{-1}) measured at 40 and 50° (HCl_{aq} concentration 12.4 mol/l) gave the following values: $k_1 = 0.003$ and 0.007 , respectively,

and $k_2 = 0.026$ and 0.030 , respectively, with root-mean-square deviations of the observations (rel. conc.) from the calculated data of 0.034 and 0.054 , respectively. It is pointed out that the molecule of H_2O formed in the second step remains trapped in the cage and only shows up as an immiscible layer on desolvation of the clathrate. This again demonstrates the ability of the clathrate lattice to accommodate small structural changes on variations of the cage contents. The chloride **3** appeared as major product at both temperatures, whereas the concentration of **2** remained roughly constant, thus pointing to a rate-determining step for the allylic conversion in accordance with the rate constants and the activation energies ΔE_1 75.3 and ΔE_2 10.9 $\text{kJ} \cdot \text{mol}^{-1}$ calculated from the above k values measured at 40° and 50° , respectively. It might be interesting to emphasize that the magnitude of the rate constants for the allylic isomerization of the enclathrated polymethyloxiranes [2] is from 60 to more than 100 times greater than that of **1**. For example, trimethyloxirane demonstrates a kinetic behavior very different from that of **1** with $k_1 = 0.870$ h^{-1} at 22° , followed by a rate-controlling HCl addition to the allylic product with a constant $k_2 = 0.032$ h^{-1} , in contrast to the *Step-b* transformation of **1**. Reactions of TOT/**1** with 48% aqueous HBr solution (HBr_{aq}) were carried out at 40° and shown to be very sluggish. The reaction mixture yielded 8% of **2** and no detectable amount of 4-bromocyclopent-2-en-1-one after 96 h. The *van der Waals* volume of the external reactant plays without doubt a role in slowing down the reaction.

As was already found for the oxirane clathrates, a slight change in the external HCl_{aq} concentration influences drastically the intracrystalline reaction rate. The relationships $k = a \cdot [\text{HCl}]^n$ was postulated between k and the concentration of HCl_{aq} , where a and n were optimized by a least-squares procedure to give $k_1 = 3.01 \cdot 10^{-7} \cdot [\text{HCl}]^4$ and $k_2 = 1.69 \cdot 10^{-5} \cdot [\text{HCl}]^3$ (Fig. 3,b). By way of example, the k_1 equation

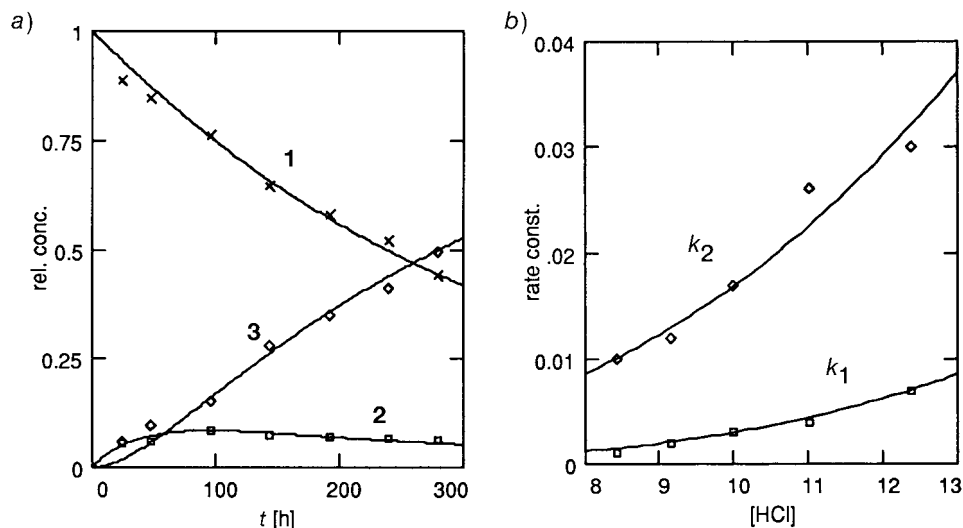


Fig. 3. a) Selected concentration-time profile of the consecutive first-order reactions $1 \rightarrow 2 \rightarrow 3$ at 40° (the integrated rate-law expressions [5] (solid curves) are fitted to the data by a least-squares procedure; concentration of HCl_{aq} 12.4 mol/l; $k_1 = 0.0029$, $k_2 = 0.0262$). b) Variations of k_1 and k_2 , as functions of the concentration of the external reactant HCl_{aq} at 50° ($[\text{HCl}]$ in mol/l; k in h^{-1}).

may be substituted for the rate constant in the first-order rate of change of **1** giving the rate expression for the first step of the heterogeneous reaction: $d[\mathbf{1}]/dt = -3.01 \cdot 10^{-7} \cdot [\mathbf{1}] \cdot [\text{HCl}]^4$, where $[\text{HCl}]$ is maintained constant. A reaction in solution is unlikely to involve the fourth power of a concentration factor, and it is believed that this high exponential dependency is due, in part, to the constitution of the outer diffusion layer at the borderline liquid-crystal. The energy of desolvation of the hydrated acid might contribute significantly to the barrier of crossing of the liquid-solid interface by a 'naked' HCl molecule, the solvation shell of the ions being likely to increase with the acid dilution.

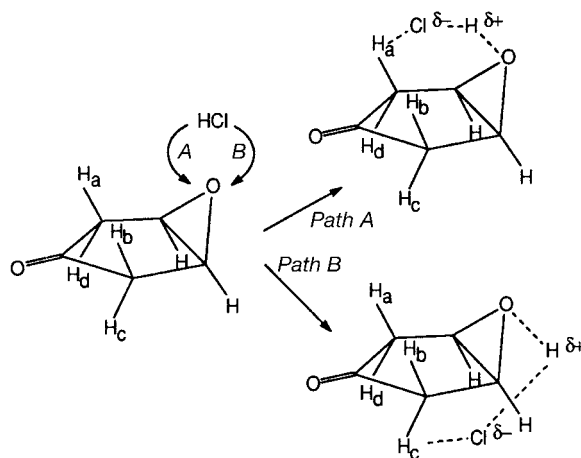
The precise treatment of kinetic data for the *solid-gas* system is not easily feasible owing to the experimental difficulty to express the 'concentration' of HCl_g in the reaction medium. The most critical part of the experimental set-up was the maintenance of a constant and homogeneous HCl_g flow through the microcrystalline conglomerate to ensure significant comparisons between the various samples. Considerable desolvation of the solid phase was encountered during the experiments; consequently, the reaction times were kept within the range from 60 to 180 h to limit the decrease of the mol contents to a maximum of *ca.* 30%. Series of three to nine reactions were carried out at three different temperatures, the kinetics agreeing with the occurrence of two successive first-order steps as for the solid-liquid system. The reaction rates (in h^{-1}) measured at 80, 100, and 120° were $k_1 \cdot 10^3 = 17 \pm 2$, 40 ± 3 , and 152 ± 5 , respectively, and $k_2 \cdot 10^3 = 15 \pm 6$, 14 ± 7 , and 12 ± 6 , respectively. The reported confidence limits, given at the 5% significance level, are those of the mean k values of series of measurements at fixed temperatures. The allylic isomerization (k_1) is considerably accelerated with an increase in temperature, the *Arrhenius* plot giving a rough estimation of the activation energy of $62 \pm 11 \text{ kJ} \cdot \text{mol}^{-1}$, a value close to that observed for the solid-liquid system. The k_2 values could only be estimated with considerable inaccuracy in comparison with the k_1 's, thus showing the limitations of the solid-gas investigations. It could only be concluded that the nucleophilic substitution $2-k_2 \rightarrow 3$ is practically temperature-independent within the range investigated.

A discussion of the possible mechanisms of the reaction of enclathrated **1** with HCl might be useful and would benefit from a simplified but convenient description of the clathrate cavity. The eight identical (*M*)-TOT molecules comprising the cavity (see *Figs. 2* and *4*) might be considered as a model for a supermolecular chiral aggregate with a C_2 axis passing through the central cavity. In a recent comprehensive study of the molecular packing of *P3₁21* clathrates, the structural features of two small entry channels leading into the central receptor were discussed and illustrated [1a][2]. They are symmetry-equivalent and situated at either end of the longest axial dimension of the cage (*ca.* 7 Å) viewed perpendicularly to *Fig. 2*. The presence of these 'channels' certainly imposes a preferred direction of attack of the incoming external reactant upon the guest.

The epoxide **1** may be protonated along two directions of attack (*Path A* or *B*, *Scheme 2*) to yield two different conjugate acids. The formal C_s symmetry of **1** entails the presence of two pairs of enantiotopic protons in α -position to the ketone function which can be abstracted by the basic Cl^- ion to produce the α,β -unsaturated alcohol and a $\text{H}^\delta+\text{Cl}^\delta-$ ion pair. Two pairs of six-membered enantiomeric transition states may be envisaged for the concerted reaction, and the stereochemical outcome depends on

which proton is attacked. It has been shown [6] that on treatment with a strong base, ring opening is prevalent consecutive to the attack on the enantiotopic proton H_a or H_b . However, a limitation to the above symmetry considerations is worth mentioning. Owing to the chiral environment and the distortion of the guest frame to fit the cage, equivalence between the α -protons is cancelled resulting in the possible occurrence of four distinct transition states. If the protonation occurs along *Path B*, the six-membered transition state would be highly unfavorable due to the prohibitive $H_c \cdots Cl^{\delta-}$ or $H_d \cdots Cl^{\delta-}$ distances and to the steric hindrance of the epoxide protons, therefore, the 'syn' mechanism along *Path A* should be favored.

Scheme 2

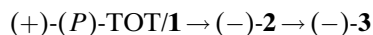


The conversion of enclathrated **1** gave optically active reaction mixtures of **2** and **3**. The presence of either one of the chiral products in the absence of the other was not obtainable as follows from the kinetics and from adverse desolvation problems at long reaction times (*Sect. 5*). A quantitative method for estimating the ee's of the products involves the relationship of *Eqn. 1* where α_{obs} is the optical activity of the reaction mixture; the c 's and $[\alpha]$'s are the concentrations and specific rotations, respectively, of the products **2** and **3**. Both coefficients c and $[\alpha]$ are experimentally accessible for **2** and **3**. Therefore, *Eqn. 1* is linear in two unknowns (ee_2 and ee_3) that can be estimated by least-squares analysis if we have a set of n such equations ($n > 2$).

$$\alpha_{\text{obs}} = ee_2 \cdot c_2 \cdot [\alpha]_2 + ee_3 \cdot c_3 \cdot [\alpha]_3 \quad (1)$$

Five small microcrystalline samples of (+)-TOT/**1** (optical purity 99.8%) [2] were reacted with HCl_g in a temperature range of 80–120° for 42–96 h. Each sample was then divided into three portions which were dissolved separately in $CDCl_3$ and analyzed by 1H -NMR spectroscopy for the concentrations of **2** and **3**; the values 91.4 and 306.8 (see *Sect. 4* and *5*) were substituted in *Eqn. 1* for $[\alpha]_2$ and $[\alpha]_3$, respectively. Besides, chiroptical measurements showed *levorotatory* (α_{obs}) reaction mixtures for every sample. Thus, we had three sets of five independent linear *Eqns. 1*, each set

yielding a best estimate for the ee's on calculation by the least-squares method. For each set, consistent results were only obtained with both coefficients $[\alpha] < 0$, disclosing unambiguously the following correlation:

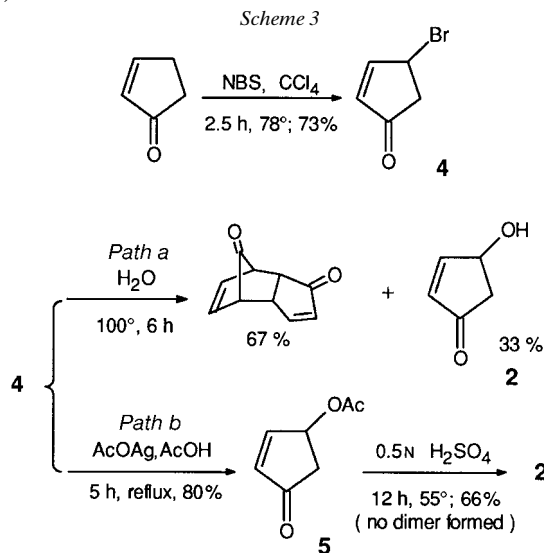


The ee's were relatively poor and not very accurately estimated, with overall values $ee_2 = 9 \pm 3\%$ and $ee_3 = 22 \pm 2\%$. According to expectations, the correlation matrix showed a large correlation between the ee's. The ee of **3**, larger than that of **2**, might reflect a leading influence of the structural differences between the diastereoisomeric associations $(P)\text{-TOT}/(S)\text{-2}$ and $(P)\text{-TOT}/(R)\text{-2}$ on the displacement of OH by Cl. Such an effect would require that $(P)\text{-TOT}/(R)\text{-2}$ favours partial inversion with respect to the couple $(P)\text{-TOT}/(S)\text{-2}$. In the present instance, one can evaluate to *ca.* 11% the fraction of $(S)\text{-3}$ formed in the chlorination step by inversion of $(R)\text{-2}$. The formation of an excess of $(S)\text{-2}$ is also consistent with its spontaneous inclusion as major enantiomer by seeding a TOT solution in racemic **2** with $(+)\text{-TOT}$ clathrate microcrystals.

In a subsequent experiment, microcrystals of $(-)\text{-TOT/1}$ of optical purity $> 99\%$ were reacted with HCl_g to yield *dextrorotatory* reaction mixtures after racemization of the host on solution in CHCl_3 . Besides, reaction products were recovered by desolvation of clathrate samples and analyzed by GC over a chiral column, showing the presence of unreacted **1** with $(+)\text{-2}$ (ee 8%) and $(+)\text{-3}$ (ee 7–8%) as major enantiomers. Chirality transfer from the cavity onto **2** is in agreement with that found previously, whereas the lower value of the ee of **3** might be accounted for by a partial inversion process on a molecule prone to racemization at higher temperature (desolvation at 180°). The correlation of optical rotations $(-)\text{-TOT/1} \rightarrow (+)\text{-2} \rightarrow (+)\text{-3}$ is complementary to that found in the preceding approach and reveals that proton abstraction from position 2 is slightly favored with respect to position 1 in *Fig. 2*. The low efficiency of the chirality transfer may be explained by the orientation of the *syn* C–H bonds, both facing the same gap of the entry channel. The proximal TOT carbonyl O-atom, apt to form the observed H-bond with the OH group, is probably a crucial orienting factor lowering the activation energy of the overall transition state involving the nearby H-atom in α -position.

3. Crystal Structure of TOT/4-Hydroxycyclopent-2-en-1-one (2) and Absolute Configuration of the Guest. – The 4-chlorocyclopent-2-en-1-one (**3**) has already been described [7], but its chiroptical properties remained unknown until now. The isolation of optically active **3** as sole product from the reaction of TOT/**1** was not possible as pointed out above. The expected inclusion method was also made impossible on account of the elusive $P3_121$ TOT/**3** clathrate (see *Sect. 5*). Consequently our attention was aimed at obtaining pure **3** by reacting TOT/**2** with HCl_{aq} . A large quantity of racemic **2** was prepared by a new pathway (*Scheme 3*) differing from that used by *Noyori* and coworkers [4]. Reaction of cyclopent-2-en-1-one with *N*-bromosuccinimide in CCl_4 afforded 4-bromocyclopent-2-en-1-one (**4**) in yields up to 73%. The conversion of **4** to **2** was accomplished by hydrolysis of either **4** or 4-acetoxycyclopent-2-en-1-one (**5**). Hydroxylation of **4** in aqueous solution (neutral, basic, or acidic) yielded the

cyclopentadiene dimer as main product in all cases (*Scheme 3, Path a*). Deacetylation of **5** with K_2CO_3 aqueous MeOH solution [8] was inappropriate because 4-methoxycyclopent-2-en-1-one was formed in 57% yield as the only identified product. On the other hand, hydrolysis of **5** gave the expected pure product **2** in acidic media, the most efficient condition (66% of **2**) being the action of aq. 0.5N H_2SO_4 at 55° (*Scheme 3, Path b*).



A challenging problem pertaining to X-ray crystal-structure analysis resides in the determination of the absolute configuration of chiral crystal components. If the *precise* recognition of the conformation of a chiral guest in $P3_121$ clathrates is at stake (unambiguous resolution of the guest atomic positions, the absolute configuration of TOT being known), the inclusion of a large excess of one of the guest enantiomers is preemprory. To avert this complication in case of low enantioselectivity of the clathrate, a substrate presenting a large ee of one of its enantiomers can be employed in the first recrystallization. Despite the fact that the enantioselectivity of TOT/**2** seemed reasonably 'high' (ee mean value $61.0 \pm 0.3\%$), optically active **2** was prepared separately *via* asymmetric synthesis. Starting with (+)-(*R,R*)-tartaric acid, (–)-(*R,R*)-1,4-diiodo-2,3-(isopropylidenedioxy)butane (57%) was obtained in four steps [9]. The diiodo derivative was allowed to react with the lithio derivative of methyl methylthiomethyl sulfoxide [10], followed by acid hydrolysis (1N $\text{H}_2\text{SO}_4/\text{Et}_2\text{O}$) affording (–)-(*S*)-**2** in 34% overall yield. The ee of (–)-**2** amounted to 78% as shown by the $^1\text{H-NMR}$ spectrum of its *Mosher* derivative [11]. Though the absolute configuration of (–)-**2** was known from a previous work of *Noyori* and coworkers [12] and from the asymmetric synthesis above, a knowledge of the structural features of TOT/**2** was important to shed light on the mechanism of the intracrystalline reaction of the guest with $\text{H}^{\delta+}\text{Cl}^{\delta-}$. The correlation (+)-TOT/(–)-**2** was demonstrated before hand by the usual polarimetric approach [1b][2]. X-Ray crystal-structure analysis was carried out on a single crystal grown from a TOT solution in (–)-**2** the ee of which was 78.8%. Single crystals selected

from the same batch revealed an average ee of 92% for included (–)-**2** owing to the phenomenon of chiral amplification [1b], a proper value for a satisfactory crystallographic structural resolution of the guest.

A stereoview of the crystal structure of the enclathrated substrate (–)-**2** is shown in Fig. 4³⁾. The guest molecular plane is approximately parallel to the vertical crystallographic twofold axis (not shown) with the carbonyl C-atom located on the axis. Interestingly, the OH group is H-bonded to one of the two TOT carbonyl O-atoms protruding into the cage. This appears to be the first observed case of one of the TOT carbonyl atoms acting as an active site in the cage and is at variance with all the other known OH-bearing TOT guests, as e.g. butan-2-ol or acetic acid. Inspection of the host-guest intermolecular contacts suggests that **2** fits snugly into the receptor as further exemplified by a fair chiral recognition (ee 61%). The well-resolved guest conformer in (+)-(*P*)-TOT/**2** had the *S*-configuration and the *levorotatory* residual optical activity after racemization of the (+)-TOT host of several clathrate crystals disclosed unambiguously the correlation of configuration (+)-(*P*)-TOT/(–)-(*S*)-**2**, and consequently the absolute configuration of **2**.

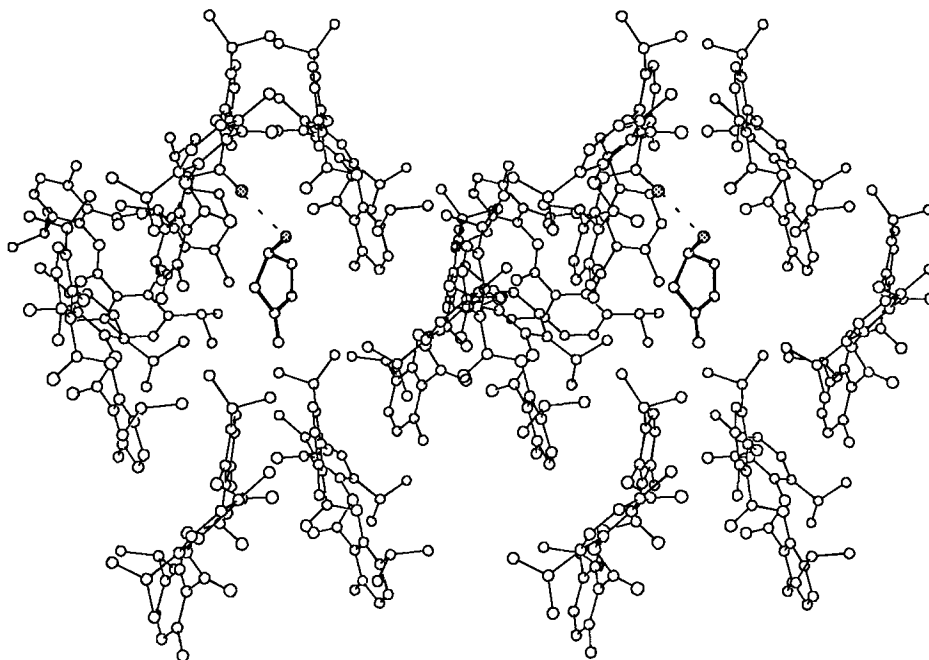


Fig. 4. Stereoview of the cage of (*M*)-TOT/(*R*)-4-hydroxycyclopent-2-enone. For clarity, the top right TOT molecule has been removed. One of the two TOT carbonyl O-atoms protruding into the cavity is H-bonded to the OH group of **2**, as depicted by the dotted line joining the solid O-atoms.

³⁾ Standardized views of the $P3_121$ cage comprising the host antipodes (–)-(*M*)-TOT have been consistently presented in our studies of TOT clathrates, thus allowing an easy comparison between the guests' orientations in different species (e.g., Figs. 2 and 4). Host-guest interactions are not affected by this approach.

4. Revised Determination of the Specific Rotation of 4-Hydroxycyclopent-2-en-1-one. – The preceding results corroborate through a different pathway the (*R*)-configuration assigned previously to (+)-**2** by *Noyori* and coworkers associated with a specific rotation $[\alpha]_D^{20}$ of +90.1 at 22° ($c=0.43$, MeOH) [12], no standard error being given. The enantiomer purity of **2** was determined by ¹H-NMR analysis of its *Mosher* derivatives ((+)-(*R*)-MTPA). The measurements were performed with samples obtained along three different pathways (*Fig. 5*): *a*) by desolvation of the microcrystalline clathrate (–)-TOT/(+)-**2** prepared from racemic **2** (ee 61.2%), *b*) by asymmetric synthesis from (*R,R*)-tartaric acid *i.e.* with (–)-**2** (ee 78.8%, *Sect. 3*), and *c*) by crystallization of the clathrate (+)-TOT/(–)-**2** on seeding with the preceding enantiomerically enriched probe (see *b*) (final ee 91.6% after desolvation). Subsequent polarimetric measurements gave access to a value for the specific rotation of **2** (*Table 1*, standard deviations at the 5% level of significance) that differ from the result of *Noyori* and coworkers. The value of the specific rotation of **2** was complemented by additional measurements in which the ee of the sample of *Fig. 5,c* was determined by GC analysis on a chiral column in association with polarimetric measurements. By the same token, this allowed configurational peak assignments in the chromatograms. Both methods delivered consistent $[\alpha]_D^{20}$ and $[\alpha]_{346}^{20}$ values in MeOH and CHCl₃.

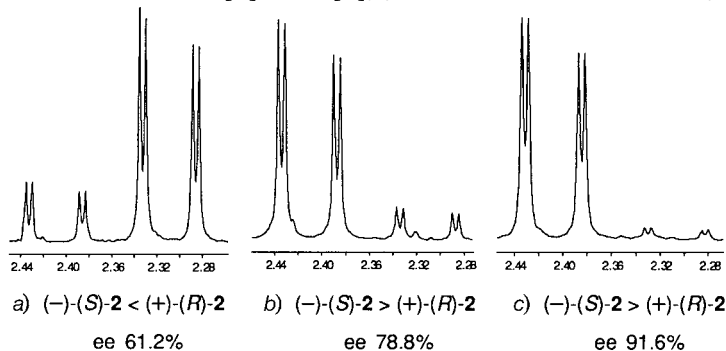


Fig. 5. Methylene ¹H-NMR signals of the *Mosher* derivatives of **2**: *a*) sample obtained after desolvation of the clathrate (–)-TOT/(+)-**2** prepared from racemic **2**; *b*) sample obtained from (–)-(S)-**2** prepared from L-tartaric acid; *c*) sample released from the clathrate (+)-TOT/(–)-**2** prepared from enantiomer-enriched (–)-(S)-**2** (ee 78.8%).

Table 1. Specific Rotation of 4-Hydroxycyclopent-2-en-1-one (**2**)

	ee [%]	$[\alpha]_D^{20}$	$[\alpha]_{346}^{20}$	Solvent
(+)-(<i>R</i>)- 2	61.2 ^a	+97.2	+100.3	MeOH
(–)-(S)- 2	78.8 ^a	–97.2	–100.8	MeOH
(–)-(S)- 2	91.6 ^b	–96.9	–100.3	MeOH
Mean $[\alpha]^{20\text{ }^c}$ ($c=2-6$, MeOH)		$\pm 97.1 \pm 0.4$	$\pm 100.5 \pm 0.7$	
(+)-(<i>R</i>)- 2	61.2 ^a	+91.3	+92.8	CHCl ₃
(–)-(S)- 2	78.8 ^a	–91.5	–93.9	CHCl ₃
(–)-(S)- 2	91.6 ^b	–91.4	–93.2	CHCl ₃
Mean $[\alpha]^{20\text{ }^c}$ ($c=2-3$, CHCl ₃)		$\pm 91.4 \pm 0.3$	$\pm 93.2 \pm 1.4$	

^a) Based on *Mosher*'s derivative. ^b) Based on *Mosher*'s derivative and GC over a chiral column (*Lipodex E*).

^c) R.m.s. errors calculated at the 5% significance level.

5. Enantiomer Enrichment of 4-Chlorocyclopent-2-en-1-one in the Solid State and Determination of its Absolute Configuration. – A knowledge of the configuration of **3** was primarily expected from the X-ray structure analysis of its TOT clathrate. Small TOT/**3** single crystals were grown in a TOT solution in the pure substrate or with (–)- α -pinene as cosolvent which afforded larger crystals. The unit cell belonged to the orthorhombic centrosymmetric space group *Pbca* ($a = 13.184$, $b = 23.086$, $c = 23.977$ Å; stoichiometric ratio TOT/**3** 1 : 1). No other crystallization conditions were found that triggered the formation of the required *P3₁21* space group, ruling out the straightforward method used for the analysis of the configuration of **2**. A different approach was used to determine the absolute configuration of **3**. Enantiomer-enriched **3** was expected from the reaction of enclathrated optically active **2** with HCl. However, (–)-**2**, ee 78% in Et₂O solution, was completely converted to racemic **3** under the action of dry gaseous HCl for 1 h at room temperature, whereas no reaction took place overnight with 20% aqueous HCl solution at the same temperature in CHCl₃. Heterogeneous reactions were preliminarily carried out making use of TOT/**2** conglomerates in the search for the proper conditions. The conversion from **2** to **3** was not complete under the most favorable reaction conditions (HCl_{aq} (38%), 53°, 110 h; molar ratio **2**/**3** 40 : 60) and exhibited to a significant extent adverse desolvation of the guests caused by the long reaction time and the higher temperature necessary to produce sizeable amounts of **3**. The slow reaction rate may be due, in part, to the host-guest H-bond (Fig. 4), the cleavage of which would increase the activation energy. Desolvation of the reacted clathrate (+)-TOT/(–)-**2** (clathrate optical purity 99%, ee of **2** 91.2%) with HCl_{aq} (38%) afforded a mixture of unreacted **2** with **3** as sole product (molar ratio **2**/**3** 1 : 3). The separation of the components of two independently reacted and desolvated crystal batches (*I* and *II*) was achieved by preparative TLC (Et₂O). This method did not cause the racemization of **3**, as demonstrated by comparing the enantiomer purity of **3** before and after separation. The ee of the samples of **3** obtained by the above treatments was determined by GC over a chiral stationary phase (Table 2, Batches *I* and *II*). The ee of (–)-**3** was 35 and 33% for the Batches *I* and *II*, respectively. The high rotatory power of **3** was determined by subsequent polarimetric measurements in CDCl₃ and MeOH.

A chemical method was employed as a last resort to specify the absolute configuration of **3**. The absolute configuration of **2** being known, the related configuration of **3** was expected from the conversion of optically active **2** to the chloride **3** under the action of thionyl chloride in the presence of an amine. This reaction is well known to induce predominantly either retention or inversion of

Table 2. Specific Rotation of 4-Chlorocyclopent-2-en-1-one (**3**) Prepared by Heterogeneous Reactions of Enclathrated (–)-(S)-**2** with HCl_{aq}^{a)}

Batch ^{b)}	ee [%] ^{c)}	$[\alpha]_{\text{D}}^{20}$	$[\alpha]_{\text{D}}^{20}$ ₅₄₆	Solvent
<i>I</i>	35	– 306.6 ± 1.5	– 368.9 ± 1.8	CDCl ₃
<i>II</i>	33	– 306.9 ± 1.5	– 368.2 ± 1.8	CDCl ₃
<i>II</i>	33	– 285.4 ± 1.4	– 342.1 ± 1.7	MeOH

^{a)} R.m.s. errors estimated at the 5% significance level. ^{b)} Chemical purity of Batches *I* and *II* after desolvation: 97.3 and 98.9%, resp. ^{c)} Measured by GC over a chiral column (*Lipodex E*).

configuration of the product depending on the participation (Et₂O, dioxane) or the absence of participation (benzene) of the solvent. The stereochemical study of the reaction of (–)-(S)-**2** (ee 78.8%) with thionyl chloride was performed in three different solvents following the procedure of *Young* and *Caserio* [13], formerly applied to the conversion of (–)-(R)-but-2-en-2-ol, a substructure of **2**. Contrary to the expected solvent-induced retention in Et₂O, the chloro derivative of the latter compound was formed predominantly with inversion of configuration. The same effect, unexpectedly, occurred during chlorination of **2** in Et₂O. This phenomenon might be imputed in both cases to the intramolecular delocalization of the positive charge developed in the reactant upon expulsion of SO₂ that minimizes the charge transfer onto the solvent while granting more migration freedom to the neighboring Cl[–] ion. The formation of a ‘long-lived’ ionic intermediate in the conversion of (–)-(R)-but-3-en-2-ol is supported by the formation of 1-chloro-but-2-ene beside (+)-(S)-3-chloro-but-2-ene, in the molar ratio 1:2 [13]. The resolution of the optically active samples of **3** was achieved by GC over a chiral column. In benzene, where structural inversion is expected, (–)-(S)-**2** gave (+)-**3** with 77% inversion, from which the conclusion could be reached that (+)-**3** corresponds to the (R)-configuration. In Et₂O, thionyl chloride gave (+)-**3** with 83% inversion, in accordance with the noteworthy behaviour of (–)-(R)-but-3-en-2-ol. In dioxane, the expected prevalent retention was observed. The results are reported in *Table 3*. Hereby, percent inversion or retention of configuration expresses the fraction of the total amount of pure enantiomer present in the starting material that underwent either one of the processes, the difference from 100% representing the contribution of the inverse process. This is at variance with the values given usually with the difference from 100% understood to be racemization. The same conclusion regarding the configuration of **3** is arrived at, when the octant rule is applied.

Table 3. *Chemical Determination of the Absolute Configuration of 4-Chlorocyclopent-2-en-1-one (3) Using the Reaction of (–)-(S)-2 with Thionyl Chloride*

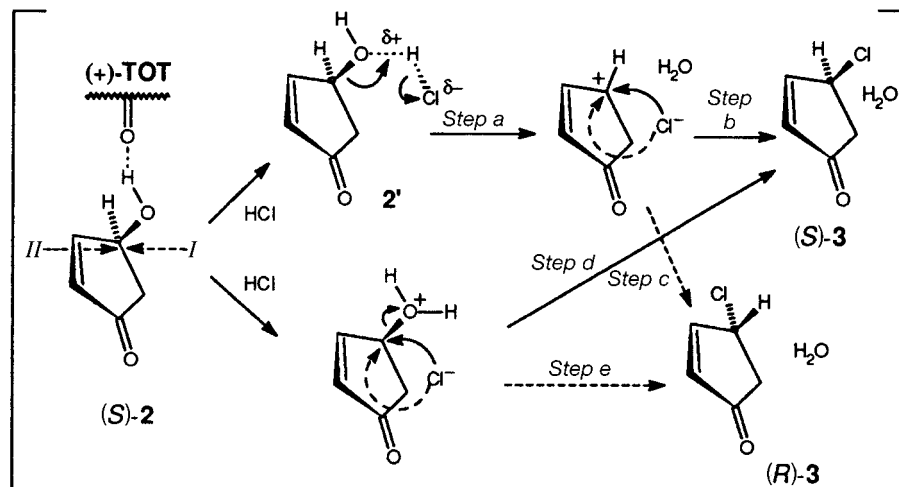
Solvent	ee [%] ^{a)}	[α] _D ^{20b)}	(CDCl ₃)	3	Stereochem. result [%] ^{c)}
Benzene	42.3	+ 313	(c = 3.6)	(+)-(R)	77 (inversion)
Et ₂ O	52.6	+ 312	(c = 1.9)	(+)-(R)	83 (inversion)
Dioxane	3.9	– 306	(c = 1.9)	(–)-(S)	52 (retention)

^{a)} % Enantiomer purity of the chloride measured by GC over a chiral column (*Lipodex E*). ^{b)} Estimated specific rotation. ^{c)} Calculated relative to the amount of enantiomerically pure alcohol initially present as reactant (see text).

The reaction of optically pure microcrystalline (+)-TOT/(–)-(S)-**2** (ee of **2** *ca.* 92%) in contact with HCl_{aq} (38%) yielded (–)-(S)-**3** with an ee of 35%, indicative of 70% retention during the conversion, as expressed by the correlation of configurations (P)-TOT/(S)-**2** → (P)-TOT/(S)-**3**. Hereby, ‘70% retention’ means that, out of 100 enclathrated (S)-**2** guest molecules, the configuration of *ca.* 70 molecules remained unchanged under the action of H^{δ+}Cl^{δ-}. On the basis of the known configurations of **2** and **3**, possible mechanisms of the reaction are depicted in *Scheme 4*. A bimolecular interaction is by nature occurring within the cage. The reaction site (C–OH moiety) of the substrate is sterically well positioned with respect to both entry channels (see *Fig. 4*), restricting the approach of the incoming reactant towards the chiral center of

(*S*)-**2** to two opposite directions: *Path I* and *II* (decrease of the entropy term). It will be noted that, owing to the H-bond between the alcohol and one of the cage carbonyl O-atoms, the facility of formation of the oxonium intermediate **2'** differs from one direction of attack to the other. Protonation along *Path I*, contrary to *Path II*, will be favored by the proper orientation of the OH lone electron pairs directed towards the incoming positive charge. The negative end of the $\text{H}^{\delta+}\text{Cl}^{\delta-}$ ion pair is likely to be positioned 'above' the ring mean plane and sterically close to the C(4)–C(5) bond. As a subsequent reaction step, the heterolytic dissociation of the C–O bond leading to a highly reactive allylic carbocation (*Step a*) might be envisaged. The fate of the carbocation is twofold depending on the side of the ring attacked by Cl^- . It is reasonable to assume that the confines of the receptor prevent a facile shift of Cl^- from one side of the ring to the other, thus favoring *Step b* (retention) at the expense of *Step c* (inversion), as was experimentally observed. The same stereochemical implications might also allow for a frontside nucleophilic attack of Cl^- on C(4) with retention of configuration (*Step d*). A $\text{S}_{\text{N}}2$ substitution with clear inversion (*Step e*) seems less likely in view of the confinement of the reactants as expressed above.

Scheme 4



Experimental Part

General. TOT was synthesized by cyclodehydration of *o*-thymotic acid with POCl_3 [1]. All solvents and reagents were purchased from high-grade commercial sources, and the solvents redistilled before use. MgSO_4 and Na_2SO_4 were employed as drying agents. Cyclopentadiene was prepared by pyrolysis of commercial dicyclopentadiene (Fluka; 85–90% by GC) and stored in a tightly capped bottle at dry-ice temperature. Et_2O was distilled from sodium benzophenone ketal (=sodium diphenylketyl) prior to use. Gaseous HCl was produced by the action of conc. sulfuric acid upon a conc. HCl soln. and dried through two traps of conc. sulfuric acid and one filled with P_2O_5 . Gaseous HBr was generated by the action of Br_2 on tetrahydronaphthalene. The precise concentrations of HCl_{aq} were titrated with 1.000N or 0.100N standard soln. of NaOH. TLC: Merck TLC silica gel 60 F_{254} plates. Gas chromatography (GC): Vega-GC-6000 capillary column (SPB 20, 30 m \times 1.0 mm), chiral column Lipodex E. Polarimetric measurements: Perkin-Elmer-241 polarimeter (accuracy: $\pm 0.002^\circ$). ^1H - (400 MHz) and ^{13}C -NMR (100.6 MHz) Spectra: Bruker-AMX-400 spectrometer; SiMe_4 as internal standard in CDCl_3 ; chemical shifts δ in ppm, J in Hz. IR Spectra: IR-Perkin-Elmer 681 using NaCl soln. cells; in cm^{-1} . Mass spectra: GV-7070 mass spectrometer with mass data system; m/z (rel. %).

Microcrystalline P3,21Clathrates. The general procedure for their preparation and desolvation were described elsewhere, as well as the method for the determination of the optical purity of the crystalline samples [1][2].

1. *Synthesis of 1. 6-Oxabicyclo[3.1.0]hex-2-ene.* Peracetic acid (40%; 126 g, 0.66 mol), previously treated with AcONa (3 g, dried), was added drop by drop to an ice-cold stirred mixture of freshly cracked cyclopentadiene (45 g, 0.68 mol) and powdered anh. Na_2CO_3 (290 g) in CH_2Cl_2 (750 ml). The temp. was maintained at 20° during the addition (ca. 1 h). After stirring for an additional 1.5 h, a starch/NaI test proved negative. The solid cake was filtered off and washed with CH_2Cl_2 (3×100 ml). The solvent was removed by distillation through a *Vigreux* column and the higher-boiling residue collected under reduced pressure in an ice-cold receiver to give 6-oxobicyclo[3.1.0]hex-2-ene (24.4 g, 59%). B.p. 38–40°/45 Torr. $^1\text{H-NMR}$: 2.31–2.68 (m, CH_2); 3.79–3.91 (m, 2 CH); 5.94–6.15 (m, 2=CH).

Cyclopent-3-en-1-one [4]. The 6-oxobicyclo[3.1.0]hex-2-ene (27 g, 0.33 mol) was added slowly to a soln. of $[\text{Pd}(\text{PPh}_3)_4]$ (50 mg, 43 mmol) in CH_2Cl_2 (80 ml) cooled in an ice bath. The reaction was highly exothermic and the temp. rose to ca. 5°. After heat evolution had ceased (ca. 4 h), the mixture yielded cyclopent-3-en-1-one (15.8 g, 95%), after flash distillation and redistillation through a *Vigreux* column. B.p. 57–61°/107 Torr. No trace of cyclopent-2-en-1-one was detected. $^1\text{H-NMR}$: 2.83 (s, 2 CH_2); 6.04 (s, 2=CH).

6-Oxabicyclo[3.1.0]hexan-3-one. (1) A mixture of cyclopent-3-en-1-one (8.2 g, 0.1 mol), NaHCO_3 (30 g), and EDTA disodium salt (=disodium dihydrogen ethylenediaminetetraacetate; 33 mg) in CH_2Cl_2 (70 ml) was treated with $\text{CF}_3\text{CO}_2\text{H}$ (prepared from 92% H_2O_2 soln. (3.9 ml, 0.15 mol) and $(\text{CF}_3\text{CO})_2\text{O}$ (24 ml, 0.17 mol) in CH_2Cl_2 (70 ml) [14]) for 15 min at 0°, then for 20 h at r.t. The reaction was quenched with $\text{Na}_2\text{S}_2\text{O}_3 \cdot 5\text{H}_2\text{O}$ (30 g) and the org. layer, together with the CH_2Cl_2 extracts (5×40 ml), dried (MgSO_4). The solvent was carefully removed under partially reduced pressure, and further distillation at 32.5–34°/0.3 Torr gave oily, pale yellow **1** (6.7 g, 68%). $^1\text{H-NMR}$: 2.49 (m, 2 CH_2); 3.76 (m, 2 CH); MS: 98 (72, M^+), 70 (100, $\text{C}_6\text{H}_6\text{O}$), 55 (42).

2. *A Novel synthesis of 2. 4-Bromocyclopent-2-en-1-one (4).* A mixture of cyclopent-2-en-1-one (50 g, 0.61 mol), *N*-bromosuccinimide (120 g, 0.67 mol), and α,α' -azodiisobutyronitrile (=2,2'-azobis[2-methylpropanenitrile]; 2.5 g) in CCl_4 (650 ml) was stirred at 77–78° for 2.5 h. After cooling in an ice-water bath, the mixture was filtered and the filter cake washed with cold CCl_4 (4×50 ml). The filtrate was washed with ice-water (3×300 ml), then with 0.1N $\text{Na}_2\text{S}_2\text{O}_3$ (300 ml), and dried (MgSO_4). After evaporation at 45°, the residual yellowish oil was distilled to yield **4** (70.3 g, 73%) which was stored at 0°. B.p. 47–48°/0.1 Torr [15]. IR (film): 1719s, 1578m, 1341m, 1178m. $^1\text{H-NMR}$: 2.71 (dd, $J = 19.5, 1.4, 1$ H, CH_2); 3.03 (dd, $J = 19.5, 6.2, 1$ H, CH_2); 5.17 (m, CHBr); 6.27 (dd, $J = 5.6, 1.2, =\text{CH}$); 7.68 (dd, $J = 5.6, 2.4, =\text{CH}$). $^{13}\text{C-NMR}$: 42.6, 44.8, 134.6, 162.2, 204.4. MS: 161 (48, M^+), 160 (50), 133 (10), 81 (100), 53 (54).

4-Acetoxy-cyclopent-2-en-1-one (5). A suspension of AcOAg (28.4 g, 0.17 mol) in a soln. of **4** (27 g, 0.168 mol) in AcOH (240 ml) was stirred under reflux for 5 h. AgBr (30 g) was filtered off and AcOH evaporated. Vacuum distillation of the residue gave **5** (18.5 g, 78%). Colorless liquid. B.p. 58–60°/0.1 Torr [15]. IR (film): 1723s, 1589w, 1373m, 1351m, 1240s, 1023s, 795m. $^1\text{H-NMR}$: 2.11 (s, Me); 2.33 (dd, $J = 18.4, 2.4, 1$ H, CH_2); 2.83 (dd, $J = 18.4, 6.4, 1$ H, CH_2); 5.86 (m, H–C(4)); 6.34 (dd, $J = 5.6, 1.2, =\text{CH}$); 7.58 (dd, $J = 5.6, 2.4, =\text{CH}$). $^{13}\text{C-NMR}$: 20.7, 40.9, 71.8, 136.9, 158.9, 170.3, 204.7. MS: 140 (29, M^+), 112 (36), 98 (100), 97 (68), 80 (37), 53 (92).

4-Hydroxycyclopent-2-en-1-one (2). A mixture of **5** (48.2 g, 0.344 mol) in 0.5N H_2SO_4 (150 ml) was stirred for 12 h at 55°. After complete disappearance of **5** ($^1\text{H-NMR}$ monitoring), the hydrolysed mixture was neutralized with Na_2CO_3 (ca. 12 g) and extracted thoroughly with Et_2O (*Soxhlet*). The combined Et_2O extracts were dried (MgSO_4) and evaporated. Distillation of the residue yielded **2** (22.5 g, 66%). Colorless oil. B.p. 62–64°/0.1 Torr. IR (film): 3392, 172, 1671, 1586, 1404, 1044. $^1\text{H-NMR}$: 2.27 (dd, $J = 2, 6.4, 1$ H); 2.77 (dd, $J = 6.4, 18.4, 1$ H); 5.05 (m, 1 H); 6.22 (dd, $J = 1.6, 5.6, 1$ H); 7.60 (dd, $J = 2, 5.6, 1$ H). MS: 98 (100, M^+), 84 (86), 70 (55).

$^1\text{H-NMR}$ signals of the *Mosher* derivatives of **2**: (+)-(R)-MTPA/(+)-(R)-**2**: 2.31 (dd, $J = 18.8, 2.2, 1$ H, CH_2); (+)-(R)-MTPA/(–)-(S)-**2**: 2.41 (dd, $J = 18.8, 2.2, 1$ H, CH_2).

3. *Racemic 4-Chlorocyclopent-2-en-1-one (3).* Anh. HCl was bubbled under vigorous stirring through a soln. of **1** (2.65 g, 0.027 mol) in CH_2Cl_2 (10 ml) for ca. 2 h at r.t.; the exothermic reaction was controlled by a cold-water bath, maintaining the temp. below 25°. The soln. was refluxed until the starting material was completely consumed ($^1\text{H-NMR}$ monitoring), then neutralized with a 7% NaHCO_3 soln. The org. layer was washed with H_2O and the aq. soln. extracted with CH_2Cl_2 . The combined org. layer and extracts were dried (MgSO_4) and evaporated. The residue was distilled under reduced pressure to yield **3** (2.25 g, 72%). Pale yellow liquid, unstable at r.t. [7]. B.p. 40–41°/1.5 Torr. IR (film): 1721.4s, 1585.4m, 1400.7, 1181.1, 792.3. $^1\text{H-NMR}$: 2.60 (dd, $J = 2, 19.2, 1$ H, CH_2); 2.98 (dd, $J = 6.8, 19.2, 1$ H, CH_2); 5.10 (m, CHCl); 6.31 (dd, $J = 1.2, 6.4, =\text{CH}$); 7.58

(*dd*, $J = 2.4, 6.4, = \text{CH}$). $^{13}\text{C-NMR}$: 44.5 (*t*); 54.2 (*d*); 135.3 (*d*); 161.3 (*d*); 204.5 (*s*). MS: 116 (42, M^+), 81 (100), 53 (73).

4. *Enantiomer Enrichment of 3*. The heterogeneous reactions of (+)-TOT/(–)-**2** with aq. HCl were performed according to the method indicated above. Desolvation was carried out at 180–185°/0.02–0.05 Torr with the volatile fraction collected at liq. N₂ temp. The separation of optically active **3** from unreacted **2** was performed by prep. TLC (Et₂O). The enantiomer purity of **3** was measured by GC (*Lipodex E*; oven temp. 100°; injector temp. 285°; detector temp. 300°).

Absolute Configuration of 3. General procedure [13]: thionyl chloride (119 mg, 1 mmol) was slowly added to a stirred soln. of (–)-(*S*)-**2** (ee 78.8%; 98 mg, 1 mmol) and tributylamine (185 mg, 1 mmol) in the adequate solvent (5 ml) as given below. The soln. was stirred at r.t., followed by evaporation. Fractionating the residue by prep. TLC (Et₂O) gave optically active **3** as a pale yellow oil. The ee's were determined as above; the specific rotations are given in Table 2. *Diethyl ether*: after 2 h stirring, 60 mg (52%) of (+)-**3**; chemical purity 97.7% by GC, ee 52.6%. *Benzene*: after 2 h stirring, 60 mg (52%) of (+)-**3**; chemical purity 96.8%; ee 42.3%. *Dioxane*: after 6 h stirring, 50 mg (45%) of (–)-**3**; chemical purity 93.8%; ee 3.9%.

Crystal-Structure Determination of TOT/1⁴. (C₃₃H₃₆O₆) · (C₅H₆O₂)_{0.5}, M_r 577.7, $\mu = 0.616 \text{ mm}^{-1}$, $F(000) = 1848$, $d_x = 1.18 \text{ g} \cdot \text{cm}^{-3}$, trigonal, $P3_121$, $Z = 6$, $a = b = 13.6602(4)$, $c = 30.304(2) \text{ \AA}$, $V = 4897.2(4) \text{ \AA}^3$; from 24 reflections ($34^\circ < 2\theta < 46^\circ$); colorless prism $0.30 \times 0.30 \times 0.28 \text{ mm}$ mounted on a quartz fiber. Cell dimensions and intensities were measured at r.t. on a *Nonius-CAD4* diffractometer with graphite-monochromated CuK $_{\alpha}$ radiation ($\lambda 1.5418 \text{ \AA}$), ω - 2θ scans, scan width $1.2^\circ + 0.14 \text{ tg } \theta$, scan speed $0.02\text{--}0.14^\circ/\text{s}$. Two reflections measured every 100 reflections showed variations less than $3.0 \sigma(I)$; $0 < h < 12$, $0 < k < 12$, $0 < l < 31$, and all antireflections of these; 3948 unique reflections were measured of which 3375 were observable ($|F_o| > 4\sigma(F_o)$). Data were corrected for *Lorentz* and polarization effects. The host structure was refined starting from the previously determined coordinates in the isomorphous TOT/but-3-en-2-ol (2 : 1) clathrate [16]. Calculations were carried out using the XTAL program [17]. ΔF syntheses revealed the major peaks of the two symmetry-equivalent guest enantiomers observable within the region of the cage after refinement of the overall model. The TOT structure was refined anisotropically by full-matrix least-squares with unit weights for the $|F|$ values; the positions of the H-atoms were calculated and included in the model with overall isotropic displacement parameters 0.060 \AA^2 ; guest atoms were refined isotropically and included with equal weight 0.30 in the structure (overall occupation factor 60%). Final values: $R = \omega R = 0.070$ and $S = 1.98$ for 378 variables and 3372 contributing reflections. The mean shift/error was $0.57 \cdot 10^{-3}$. The final difference electron density map showed a maximum of $+0.46$ and a minimum of -0.27 e\AA^{-3} .

Crystal Structure Determination of TOT/2⁴. (C₃₃H₃₆O₆) · (C₅H₆O₂)_{0.5}, M_r 577.7, $\mu = 0.616 \text{ mm}^{-1}$, $F(000) = 1848$, $d_x = 1.17 \text{ g} \cdot \text{cm}^{-3}$, trigonal, $P3_121$, $Z = 6$, $a = b = 13.7649(5)$, $c = 30.057(2) \text{ \AA}$, $V = 4932.0(4) \text{ \AA}^3$; from 24 reflections ($34^\circ < 2\theta < 46^\circ$); colorless prism $0.22 \times 0.25 \times 0.35 \text{ mm}$ mounted on a quartz fiber. Cell dimension and intensity measurements and data reduction were performed under conditions identical to those used for **1**. Of the 3971 unique reflections measured, 3082 were observable ($|F_o| > 4\sigma(F_o)$). The approach to the crystal-structure determination was the same as that for **1**. A minimum-energy conformation was calculated for **2** by the force-field method (MM2 program [18]). The (+)-(*R*)-molecule was initially positioned on the sites revealed by ΔF syntheses within the region of the cage after refinement of TOT alone. The TOT structure was refined anisotropically by full-matrix least-squares with unit weights for the $|F|$ values; the positions of the H-atoms were calculated and included in the model with overall isotropic displacement parameters 0.060 \AA^2 . The guest atoms positions were refined isotropically applying restraints on bond lengths and angles and included with equal occupation factor 0.30 in the structure (measured guest occupation factor in the clathrate 61%). Final values: $R = \omega R = 0.077$ and $S = 2.38$ for 381 variables and 3971 contributing reflections. The mean shift/error was $0.31 \cdot 10^{-2}$. The final difference electron density map showed a maximum of $+0.56$ and a minimum of -0.29 e\AA^{-3} .

⁴) Crystallographic data have been deposited with the *Cambridge Crystallographic Data Center*, University Chemical Laboratory, 12 Union Road Cambridge CB21EZ, England. The $P3_121$ TOT clathrates are isomorphous, and the coordinates of the host atoms are very similar in all species studied. A typical coordinates set is given in [16].

REFERENCES

- [1] a) R. Gerdil, in 'Comprehensive Supramolecular Chemistry', Vol. 6, 'Solid-State Supramolecular Chemistry: Crystal Engineering', Ed. D. D. MacNicol, F. Toda, and R. Bishop, Elsevier Science Ltd, Oxford, 1996, p. 239–280; b) R. Gerdil, in 'Topics in Current Chemistry', Ed. E. Weber, Springer-Verlag, Berlin-Heidelberg, 1987, Vol. 140, p. 75–105.
- [2] R. Gerdil, G. Barchietto, *Helv. Chim. Acta* **1994**, *77*, 691.
- [3] M. Bartók, K. L. Láng, in 'Heterocyclic Compounds, Small Ring Heterocycles', Part 3, 'Oxiranes', Ed. A. Hassner, Wiley, New York, 1986, Vol. 42, p. 1–196.
- [4] M. Suzuki, Y. Oda, R. Noyori, *J. Am. Chem. Soc.* **1979**, *101*, 1623.
- [5] K. B. Wiberg, in 'Physical Organic Chemistry', John Wiley & Sons, Inc., New York, 1964.
- [6] R. P. Thummel, B. Rickborn, *J. Am. Chem. Soc.* **1970**, *92*, 2064.
- [7] B. W. Ponder, D. R. Walker, *J. Org. Chem.* **1967**, *32*, 4136.
- [8] D. Bianchi, P. Cesti, E. Battistel, *J. Org. Chem.* **1988**, *53*, 5531.
- [9] K. Ogura, M. Yamashita, G. Tsuchihashi, *Tetrahedron Lett.* **1976**, 759; T. Tanaka, S. Kurozumi, T. Toru, S. Miura, M. Kobayashi, S. Ishimoto, *Tetrahedron* **1976**, *32*, 1713; M. Kitamura, K. Manabe, R. Noyori, H. Takaya, *Tetrahedron Lett.* **1987**, *28*, 4719.
- [10] K. Ogura, M. Yamashita, M. Suzuki, G. Tsuchihashi, *Tetrahedron Lett.* **1974**, 3653; K. Ogura, M. Yamashita, S. Furukawa, M. Suzuki, G. Tsuchihashi, *ibid.* **1975**, 2767.
- [11] J. A. Dale, D. L. Dull, H. S. Mosher, *J. Org. Chem.* **1969**, *34*, 2543.
- [12] M. Suzuki, T. Kawagishi, A. Yanagissawa, T. Suzuki, N. Okamura, R. Noyori, *Bull. Chem. Soc. Jpn.* **1988**, *61*, 1299.
- [13] W. G. Young, F. F. Caserio Jr., *J. Org. Chem.* **1961**, *26*, 245.
- [14] W. D. Emmons, *J. Am. Chem. Soc.* **1954**, *76*, 3468.
- [15] C. H. DePuy, M. Isaks, K. L. Eilers, G. F. Morris, *J. Org. Chem.* **1964**, *29*, 3503.
- [16] J. Siripitayananon, R. Gerdil, *Acta Crystallogr., Sect. C* **1989**, *45*, 768.
- [17] S. R. Hall, H. D. Flack, J. M. Steward, 'XTAL 3.2 User's Manual', Universities of Western Australia and Maryland, 1992.
- [18] N. L. Allinger, *J. Am. Chem. Soc.* **1977**, *99*, 8127.

Received December 23, 1998